COMMUNICATION

ChemComm
www.rsc.org/chemcomm

Low-temperature synthesis of titanium disulfide nanotubes

Jun Chen,* Suo-Long Li, Zhan-Liang Tao and Feng Gao
Institute of New Energy Material Chemistry, Nankai University, Tianjin 300071, P.R. China.
E-mail: chenabc@nankai.edu.cn

Received (in Cambridge, UK) 7th January 2003, Accepted 28th February 2003
First published as an Advance Article on the web 18th March 2003

A low-temperature gas reaction was used to successfully synthesize TiS_2 nanotubes with an outer diameter of ~20 nm, an inner diameter of ~10 nm, an interlayer spacing of ~0.57 nm, and an average length of 2–5 μm.

There is growing interest in the synthesis, characterization, and application of inorganic nanomaterials. Using the paradigm of carbon fullerenes, Tenne *et al.* first described that nanoparticles of 2-D layered metal dichalcogenide compounds such as WS_2 and MoS_2 would not retain their flat structure and collapse into fullerene-like cages and nanotubes through a gas–solid reaction at high temperatures (800–950 °C).[1,2] Various strategies and techniques have been developed or adopted to prepare nanostructural Group 6 metal chalogenides including sulfides, selenides, and tellurides.[3–9] Following the observations of 2-D layered metal disulfide nanotubes, Nath and Rao used Group 5 and Group 4 metal trisulfides as starting materials to synthesize nanotubes of layered metal disulfides at high temperatures of 800–1000 °C.[10,11] However, compared to the stable HfS_2 and ZrS_2 nanotubes, TiS_2 nanotubes were more electron beam sensitive.[11] Herein we report that high-purity TiS_2 nanotubes (1T symmetry) can be synthesized through another method, which involved heating $TiCl_4$, H_2, and H_2S inside a furnace at a relatively low temperature of 450 °C.

The operations of the present experimental reactions were carried out in the rigorous absence of oxygen and water. Titanium(IV) chloride ($TiCl_4$, 99.9%) was supplied by Aldrich. The fluxes of $TiCl_4$ flowed by pure hydrogen gas, which were automatically controlled by mass-flow meters, were introduced into a horizontal stainless steel furnace. At the same time, H_2S (ratio $TiCl_4:H_2S$ = 1:1) was induced through a tube into the reactor. The venting gases were treated with 2 M $ZnSO_4$ solutions for friendly environmental emission. We found that an inlet mixing gas flow rate of 80 mL min^{-1} and a heating temperature of 450 °C for 30 min, which shifted the chemical equilibrium in favor of TiS_2 (Eqn. 1), yielded the best and most reproducible results (about 1 g per 30 min). After the reaction was completed, the resulting black-brown solid was filtered, washed with deionized water, and finally dried in a vacuum at 80 °C for 1 h.

The as-synthesized samples were characterized by X-ray powder diffraction (XRD, Rigaku INT-2000), X-ray photoelectron spectroscopy (XPS, Shimadzu ESCA-3400), transmission electron microscopy (TEM, Philips Tecnai F20), and Brunauer–Emmett–Teller (BET, Shimadzu ASAP 2010) nitrogen sorption measurement. After these investigations, we were able to obtain titanium disulfide nanotubes by the reaction expressed as

$$TiCl_4 + 2H_2S \rightarrow TiS_2 + 4HCl \quad (1)$$

The XRD pattern of the product compares well to the known one for polystalline TiS_2 (ICDD-JCPDS No. 15-0853). Although the peaks are relatively broadened, they can be indexed to the hexagonal structure with calculated cell parameters a = 3.4052(2) Å and c = 5.6968(4) Å. The mean crystal size estimated from the Debye–Scherrer formation on the (001) reflection is about 2 nm.

The electronic binding energy spectra of Ti and S in the as-prepared product are shown in Fig. 1a and b, respectively. The binding energies are characteristic of well-defined spin-coupled Ti ($2p_{3/2}$, $2p_{1/2}$) and S ($2p_{3/2}$, $2p_{1/2}$) doublets, consistent with that of conventional TiS_2.[12] Analyses of the Ti (2p) and S (2p) peak areas gave a Ti/S atomic ratio of 1:2, indicating that the chemical composition of the final product is TiS_2.

The TEM images of the layered TiS_2 nanotubes are shown in Fig. 2. Typical TEM images at low magnification in Fig. 2a and

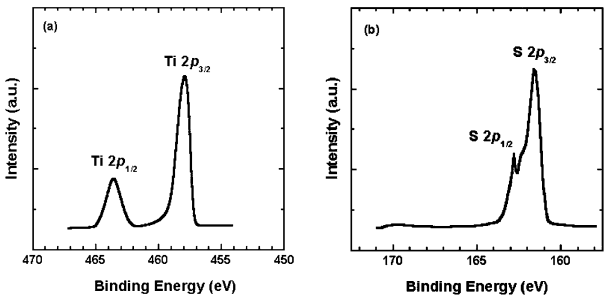

Fig. 1 XPS spectra for (a) Ti 2p and (b) S 2p of the as-synthesized product through the low-temperature heating process.

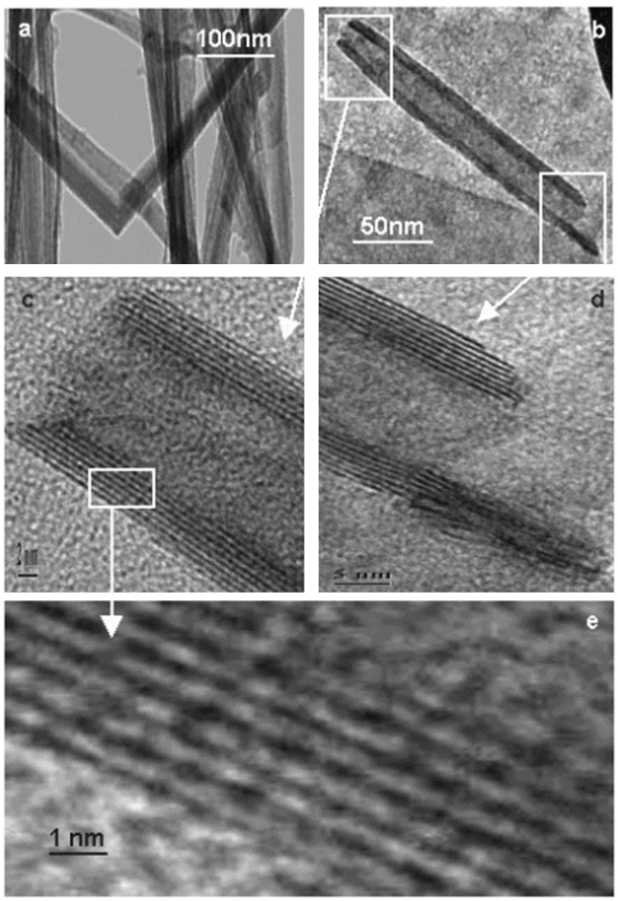

Fig. 2 TEM and HRTEM images of the as-synthesized TiS_2 nanotubes: (a, b) low-magnification TEM images and (c, d, e) HRTEM images.

DOI: 10.1039/b300054k

b show that the products are curved nanotubes and that the yield of nanotubes is quite high (> 90%). The high-resolution TEM (HRTEM) images in Fig. 2c and d demonstrate that the nanotubes are hollow and that the tube tips are open. The outer diameter of a typical hollow tube is ~20 nm, while the inner diameter is ~10 nm. The average distance between two neighboring fringes is ~0.57 nm, which means that the unit cell consists of one layer with interlayer spacing of ~0.57 nm due to the fact that TiS_2 belongs to the lamellar materials with octahedral arrangements of the S atoms around the Ti atoms.[13] Moreover, various defects such as short terminations and boundaries were found in the nanotube walls (Fig. 2e), possibly owing to the occurrence of an extra sulfur (or titanium) atom in the middle of hexagonal rings. The TiS_2 nanotubes are not sensitive to electron beam irradiation during the HRTEM investigation.

The growth of TiS_2 nanotubes yields mesoporous channel walls with large hysteresis loops that resemble typical H_2-type nitrogen adsorption/desorption isotherms (Fig. 3). The strong hysteresis is believed to be related to the capillary condensation associated with large pore channels and/or cages.[14] Barrett–Joyner–Halenda (BJH) analyses illustrate that the as-synthesized TiS_2 nanotubes exhibit a mean pore size of 25 Å (2.5 nm, inset of Fig. 3) with a surface area of 18.5 $m^2\ g^{-1}$.

In summary, TiS_2 nanotubes can be generated from heating $TiCl_4$ (flowed with H_2) in an H_2S atmosphere. The structure, morphology, and N_2 adsorption–desorption isotherms of the as-synthesized TiS_2 nanotubes are also characterized. The results show that the present route can produce pure multiwalled TiS_2 nanotubes with open-ended tips.

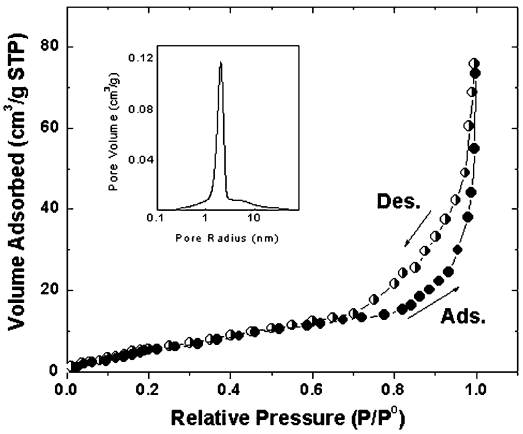

Fig. 3 Nitrogen adsorption–desorption isotherms and BJH pore size distribution curve (inset) for the as-synthesized TiS_2 nanotubes.

This work was supported by the Trans-Century Training Programme Foundation for the Talents by the State Ministry of Education.

Notes and references

1 R. Tenne, L. Margulis, M. Genut and G. Hodes, *Nature*, 1992, **360**, 444.
2 L. Margulis, G. Salitra and R. Tenne, *Nature*, 1993, **365**, 113.
3 (*a*) M. Hershfinkel, L. A. Gheber, V. Volterra, J. L. Hutchison, L. Margulis and R. Tenne, *J. Am. Chem. Soc.*, 1994, **116**, 1914; (*b*) Y. Feldman, E. Wasserman, D. J. Srolovitz and R. Tenne, *Science*, 1995, **267**, 222; (*c*) R. Tenne, *Adv. Mater.*, 1995, **7**, 965; (*d*) R. Tenne, M. Homyonfer and Y. Feldman, *Chem. Mater.*, 1998, **11**, 3225.
4 (*a*) D. H. Galván, J. H. Kim, M. B. Maple, M. Avalos-Borja and E. Adem, *Fullerene Sci. Technol.*, 2000, **8**, 143; (*b*) D. H. Galván, J. H. Kim, M. B. Maple and E. Adem, *Fullerene Sci. Technol.*, 2001, **9**, 225.
5 (*a*) M. Remskar, Z. Skraba, M. Regula, C. Ballif, R. Sanjines and F. Lévy, *Adv. Mater.*, 1998, **10**, 246; (*b*) M. Remskar, A. Mrzel, Z. Skraba, A. Jesih, M. Ceh, J. Demsar, P. Stadelmann, F. Lévy and D. Mihailovic, *Science*, 2001, **292**, 479.
6 (*a*) C. M. Zelenski and P. K. Dorhout, *J. Am. Chem. Soc.*, 1998, **120**, 734; (*b*) H. W. Liao, Y. F. Wang, S. Y. Zhang and Y. T. Qian, *Chem. Mater.*, 2001, **13**, 6.
7 (*a*) Y. Q. Zhu, W. K. Hsu, N. Grobert, B. H. Chang, M. Terrones, H. Terrones, H. W. Kroto and D. R. M. Walton, *Chem. Mater.*, 2000, **12**, 1190; (*b*) Y. Q. Zhu, W. K. Hsu, M. Terrones, S. Firth, N. Grobert, R. J. H. Clark, H. W. Kroto and D. R. M. Walton, *Chem. Commun.*, 2001, 121.
8 (*a*) J. Chen, N. Kuriyama, H. T. Yuan, H. T. Takeshita and T. Sakai, *J. Am. Chem. Soc.*, 2001, **123**, 11813; (*b*) J. Chen, S. L. Li, Q. Xu and K. Tanaka, *Chem. Commun.*, 2002, 1722; (*c*) J. Chen, S. L. Li, F. Gao and Z. L. Tao, *Chem. Mater.*, 2003, **15**, 1012.
9 (*a*) M. Nath, A. Govindaraj and C. N. R. Rao, *Adv. Mater.*, 2001, **13**, 283; (*b*) M. Nath and C. N. R. Rao, *Chem. Commun.*, 2001, 2236.
10 M. Nath and C. N. R. Rao, *J. Am. Chem. Soc.*, 2001, **123**, 4841.
11 M. Nath and C. N. R. Rao, *Angew. Chem., Int. Ed.*, 2002, **41**, 3451.
12 D. Briggs and M. P. Seah, *Practical Surface Analysis – Auger and X-ray Photoelectron Spectroscopy*, John Wiley & Sons, Chichester, 1990.
13 The salient structural features of TiS_2 are blocks of two hexagonally closed-packed chalcogen layers between which Ti metals reside in octahedral coordination of six chalcogens, whereas the MS_2 (M = Mo or W) units are arranged in a trigonal prismatic structure (prismatic coordination of six chalcogens), see J. A. Wilson and A. D. Yoffe, *Adv. Phys.*, 1969, **18**, 193.
14 S. J. Gregg and K. S. W. Sing, *Adsorption, Surface Area and Porosity*, Academic Press, London, 1997.